

This article was downloaded by:

On: 25 January 2011

Access details: *Access Details: Free Access*

Publisher *Taylor & Francis*

Informa Ltd Registered in England and Wales Registered Number: 1072954 Registered office: Mortimer House, 37-41 Mortimer Street, London W1T 3JH, UK



Liquid Crystals

Publication details, including instructions for authors and subscription information:

<http://www.informaworld.com/smpp/title~content=t713926090>

Mesomorphism of complexed 2,6-disubstituted pyridine ligands: crystal and molecular structure of two bent-core pyridines

Mari Carmen Torralba^a; Deborah M. Huck^{ab}; H. Loc Nguyen^a; Peter N. Horton^c; Bertrand Donnio^b; Michael B. Hursthouse^c; Duncan W. Bruce^d

^a Department of Chemistry, University of Exeter, Exeter EX4 4QD, UK ^b IPC MS, UMR 7504 (CNRS-ULP), GMO, 23 rue du Loess, BP 43, 67034 Strasbourg Cedex 2, France ^c EPSRC Crystallographic Service, Department of Chemistry, University of Southampton, Highfield, Southampton SO17 1BJ, UK

^d Department of Chemistry, University of York, Heslington, YORK YO10 5DD, UK

To cite this Article Torralba, Mari Carmen , Huck, Deborah M. , Nguyen, H. Loc , Horton, Peter N. , Donnio, Bertrand , Hursthouse, Michael B. and Bruce, Duncan W.(2006) 'Mesomorphism of complexed 2,6-disubstituted pyridine ligands: crystal and molecular structure of two bent-core pyridines', *Liquid Crystals*, 33: 4, 399 – 407

To link to this Article: DOI: 10.1080/02678290600633485

URL: <http://dx.doi.org/10.1080/02678290600633485>

PLEASE SCROLL DOWN FOR ARTICLE

Full terms and conditions of use: <http://www.informaworld.com/terms-and-conditions-of-access.pdf>

This article may be used for research, teaching and private study purposes. Any substantial or systematic reproduction, re-distribution, re-selling, loan or sub-licensing, systematic supply or distribution in any form to anyone is expressly forbidden.

The publisher does not give any warranty express or implied or make any representation that the contents will be complete or accurate or up to date. The accuracy of any instructions, formulae and drug doses should be independently verified with primary sources. The publisher shall not be liable for any loss, actions, claims, proceedings, demand or costs or damages whatsoever or howsoever caused arising directly or indirectly in connection with or arising out of the use of this material.

Mesomorphism of complexed 2,6-disubstituted pyridine ligands: crystal and molecular structure of two bent-core pyridines

MARI CARMEN TORRALBA†, DEBORAH M. HUCK†‡, H. LOC NGUYEN†, PETER N. HORTON§, BERTRAND DONNIO‡, MICHAEL B. HURSTHOUSE§ and DUNCAN W. BRUCE*¶

†Department of Chemistry, University of Exeter, Stocker Road, Exeter EX4 4QD, UK

‡IPC MS, UMR 7504 (CNRS–ULP), GMO, 23 rue du Loess, BP 43, 67034 Strasbourg Cedex 2, France

§EPSRC Crystallographic Service, Department of Chemistry, University of Southampton, Highfield, Southampton SO17 1BJ, UK

¶Department of Chemistry, University of York, Heslington, YORK YO10 5DD, UK

(Received 22 December 2005; accepted 31 January 2006)

Bent-core, polycatenar pyridines are reported, synthesized via a Siegrist coupling of di- and tri-alkoxybenzylidene fragments with 2,6-dimethylpyridine. None of these pyridines was liquid crystalline. Isomeric materials based on a 3,5-disubstituted pyridine core were mesomorphic in hydrogen-bonded complexes, whereas these new materials were not. However, the new pyridines did form mesomorphic metal complexes with silver salts. Some insight into this behaviour is gleaned from single crystal structure determinations of the model systems, 3,5-bis(3',4'-dimethoxystyryl)pyridine and 2,6-bis(3',4'-dimethoxystyryl)pyridine.

1. Introduction

Over several years, we have reported on the liquid crystal chemistry of stilbazoles [1], their metal complexes [2], hydrogen- and halogen-bonded complexes [1, 3] and their behaviour as NLO chromophores [4] and as materials for Langmuir–Blodgett film formation [1, 5]. This work has proved extremely fruitful, and recently we showed how the chemistry that describes these stilbazole systems may be extended to produce the polycatenar 3,5-disubstituted pyridines (figure 1: **1**) and their related silver(I) complexes (figure 1: **2**) [6], which may also formally be regarded as bent-core mesogens [7]. These pyridines were prepared using the Siegrist methodology [8] that required reaction of 3,5-dimethylpyridine with a source of the di- or tri-alkoxybenzylidene fragment, provided in this case via the related imine. This led cleanly to the disubstituted product in which the *E*-isomer was obtained for each double bond as shown by the J_{AB} coupling constant which was found to be around 16 Hz.

2,6-Dimethylpyridine is available in addition to its 3,5-isomer, and indeed has been used recently in the construction of extended, polycatenar, bent-core mesogens [9]. This 2,6-isomer differs significantly from the

3,5-analogue in that the proximity of the groups in the 2- and 6-positions can compromise access to the pyridine nitrogen, and this made us curious to synthesize 2,6-equivalents of **1** and to see how their liquid crystal properties and complexation ability might vary.

As shown in figure 2, the synthesis of these new pyridines followed a route analogous to that employed for the 3,5-predecessors, once more employing Siegrist chemistry. The off-white compounds were recovered in yields of between 61 and 85%, and were characterized by ^1H NMR spectroscopy, which showed a triplet and a doublet at δ 7.65 and 7.28, respectively for the protons on the pyridyl ring, and an AB system that confirmed the *trans* nature of the double bond with a coupling constant of 16.0 Hz. Interestingly, the chemical shift of the vinylic hydrogen β to the pyridyl ring in the 2,6-isomers is shifted by 0.5 ppm to higher frequency compared with that found in the 3,5-isomer (from δ 7.13 to 7.63), which we attribute to the fact that in the 2,6-isomers, the styryl groups are in conjugation with the ring nitrogen.

2. Crystal and molecular structure of 2,6-di(3',4'-dimethoxystyryl)pyridine and 3,5-di(3',4'-dimethoxystyryl)pyridine

In order to obtain more detailed information about the conformation of these new 2,6-disubstituted pyridines

*Corresponding author. Email: db519@york.ac.uk

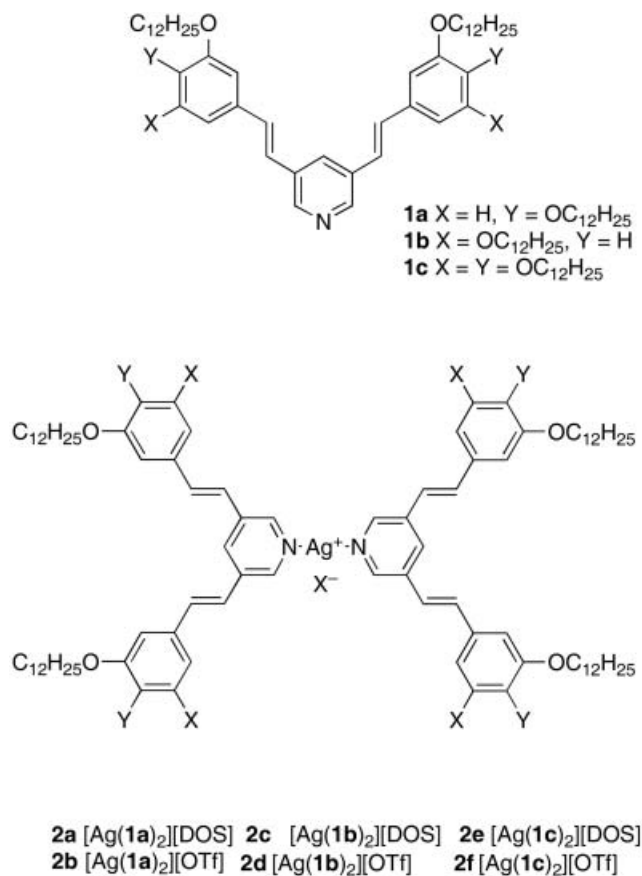


Figure 1. Structures of the ligands and complexes reported previously.

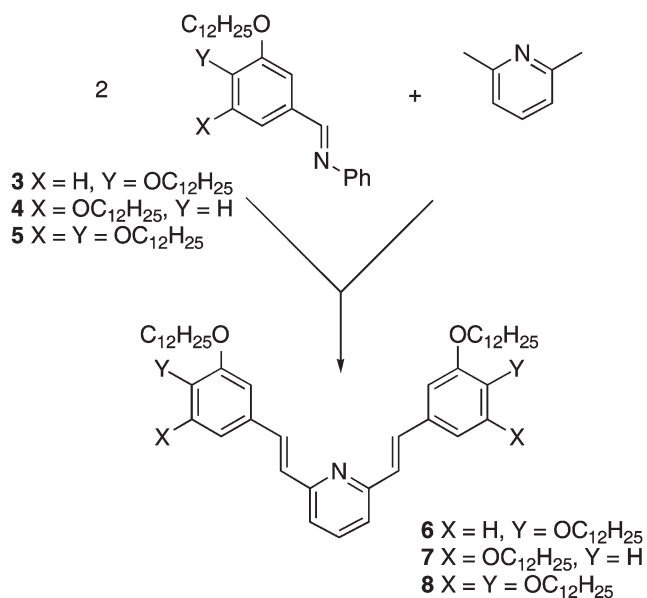


Figure 2. Synthesis of the 2,6-disubstituted pyridines.

and to compare them with the 3,5-analogues, single crystals were grown of both isomers substituted using a 3,4-dimethoxystyryl function, the shorter chains aiding crystallization. Structure refinement parameters and crystal data are summarized in table 1.

Three views of the molecular structure of the 2,6-isomer, which crystallized in an orthorhombic system, are shown in figure 3 where it can be seen that the molecule is essentially planar, the two torsional angles between the styryl double bonds and the pyridine ring being *c.* 2.6° and 5.7° out of plane, while the angles between the central pyridine ring and the corresponding dimethoxyphenyl units are 16.4(1)° and 13.2(1)°, respectively. What is apparent immediately is that the two double bonds have a different disposition with respect to the pyridine ring, even though both have an *E*-configuration. We believe that this is due to the steric requirements of the non-bonded pair of electrons associated with the pyridyl nitrogen, which prevent both double bonds adopting what we might call an 'in-in' arrangement that would lead to severe steric crowding. Indeed, figure 3(c) is a space-filling model that shows the resulting availability of the nitrogen quite well; of course, this availability would be enhanced if the two styryl groups twisted out of plane. The ¹H NMR spectrum, however, showed only one set of signals corresponding to an AB system, which is probably due to free rotation of the arms of the molecule in solution, resulting in averaged signals being detected.

Three views of the molecular structure of the 3,5-isomer, which crystallized in a monoclinic system, are shown in figure 4 where it can be seen that the molecule is essentially planar. However, the steric effect of the pyridyl C–H appears significantly smaller than that of the nitrogen lone pair as in this case both styryl double bonds have adopted the same 'in-in' arrangement, and what steric strain there is has been relieved by one styryl arm twisting to give a torsional angle to the ring of 20.5°, with the other closer to planarity at 4.5°. Corresponding angles between the central pyridine and the dimethoxyphenyl group are 10.9(2)° and 20.3(2)°, respectively.

3. Mesomorphic Properties

3.1. Pure ligands

Unlike the situation for the 3,5-disubstituted systems where the hexacatenar derivative, **1c**, was mesomorphic, none of the new pyridines showed any liquid crystal phases, rather melting to the isotropic liquid at 84°C (**6**), 64°C (**7**) and 60°C (**8**). These melting points are comparable to those of **1**.

Table 1. Structure refinement parameters and crystal data.

Parameter	2,6-Isomer	3,5-Isomer
Empirical formula	C ₂₅ H ₂₅ NO ₄	C ₂₅ H ₂₅ NO ₄
Formula weight	403.46 g mol ⁻¹	403.46 g mol ⁻¹
Temperature	120(2) K	15(2) K
Wavelength	0.71073 Å	0.71073 Å
Crystal system	Orthorhombic	Monoclinic
Space group	<i>P</i> 2 ₁ 2 ₁ 2 ₁	<i>P</i> 2 ₁
Unit cell dimensions	<i>a</i> =7.7425(2) Å α =90.000(5)° <i>b</i> =9.4609(2) Å β =90.000(5)° <i>c</i> =28.8094(9) Å γ =90.000(5)°	<i>a</i> =11.462(2) Å α =90° <i>b</i> =5.4768(11) Å β =108.58(3)° <i>c</i> =17.641(4) Å γ =90°
Volume	2110.32(10) Å ³	1049.7(4) Å ³
<i>Z</i>	4	2
Density (calculated)	1.270 Mg m ⁻³	1.277 Mg m ⁻³
Absorption coefficient	0.086 mm ⁻¹	0.086 mm ⁻¹
<i>F</i> (000)	856	428
Crystal	Shard; pale orange	Colourless plate
Crystal size	0.45 × 0.32 × 0.10 mm ³	0.48 × 0.18 × 0.05 mm ³
θ range for data collection	3.02–27.47°	5.12–27.48°
Index ranges	−9 ≤ <i>h</i> ≤ 10, −10 ≤ <i>k</i> ≤ 12, −24 ≤ <i>l</i> ≤ 37	−11 ≤ <i>h</i> ≤ 14, −7 ≤ <i>k</i> ≤ 5, −21 ≤ <i>l</i> ≤ 22
Reflections collected	12978	4339
Independent reflections	2760 [<i>R</i> _{int} =0.0584]	2283 [<i>R</i> _{int} =0.0560]
Completeness to θ =27.47°	99.3%	86.2%
Absorption correction	Semi-empirical from equivalents	Semi-empirical from equivalents
Max. and min. transmission	0.9915 and 0.9624	0.9957 and 0.9598
Refinement method	Full-matrix least-squares on <i>F</i> ²	Full-matrix least-squares on <i>F</i> ²
Data/restraints/parameters	2760/0/276	2283/1/275
Goodness-of-fit on <i>F</i> ²	1.125	1.097
Final <i>R</i> indices [<i>F</i> ² >2σ(<i>F</i> ²)]	<i>R</i> 1=0.0385, <i>wR</i> 2=0.0795	<i>R</i> 1=0.0527, <i>wR</i> 2=0.1300
<i>R</i> indices (all data)	<i>R</i> 1=0.0532, <i>wR</i> 2=0.0849	<i>R</i> 1=0.0666, <i>wR</i> 2=0.1389
Absolute structure parameter	not determined reliably	not determined reliably
Largest diff. peak and hole	0.188 and −0.157 e Å ⁻³	0.296 and −0.303 e Å ⁻³

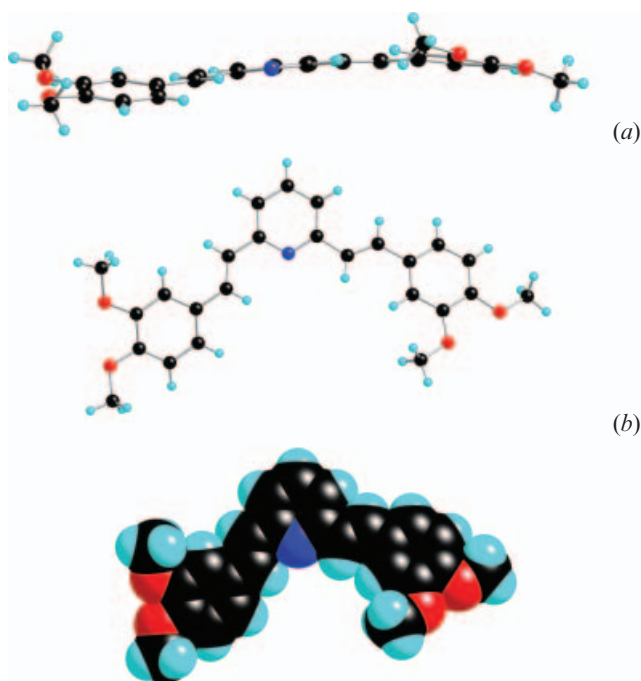


Figure 3. Three views of the molecular structure of 2,6-di(3',4'-dimethoxystyryl)pyridine.

3.2. Hydrogen-bonded complexes

Pyridine-based ligands such as stilbazole derivatives are hydrogen-bonding acceptors and complexation of various stilbazoles with different hydrogen-bonding donors has shown that hydrogen-bonding interactions can induce mesomorphic properties [10]. Given that the pyridine nitrogen of compounds **6** to **8** is less accessible than that of the 3,5-isomer, we decided first to examine the formation of some hydrogen-bonded complexes as we were confident that a proton would certainly be able to approach the nitrogen.

We first prepared hydrogen-bonded complexes (figure 5) of the 3,5-compound **1c**, with 4-dodecyloxybenzoic acid (**9**) and 3,4,5-trioctyloxybenzoic acid (**10**) to act as a point of reference. The complexes were prepared by dissolving each component separately in THF and then adding the two solutions together. The solution was stirred for an hour and the solvent removed on a rotary evaporator. Subsequent investigation by DSC and microscopy revealed that thermal annealing was required for complex formation and to obtain reproducible mesomorphism, a phenomenon that we have observed before [11].

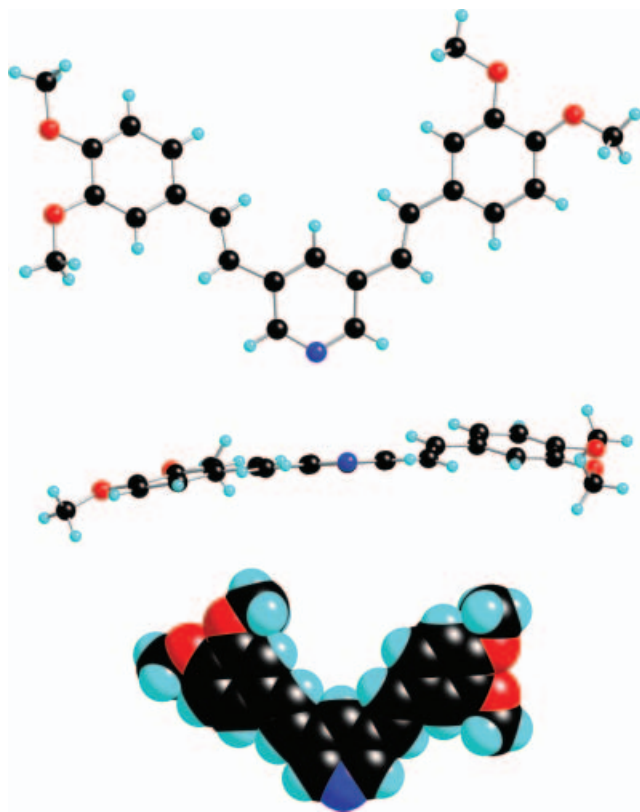


Figure 4. Three views of the molecular structure of 3,5-di(3',4'-dimethoxystyryl)pyridine.

The two complexes were studied by polarising optical microscopy (POM), DSC and X-ray diffraction (XRD) and were found to be mesomorphic. The first heating cycle was complicated because this was when complexation occurred, and on cooling only one peak was observed in the DSC trace as a result of the isotropic-to-columnar phase transition, after which the complexes formed a glass. On second heating, the glass-to-columnar phase transition was not detected by DSC,

so only the columnar phase-to-isotropic transitions are presented in table 2.

The complex with 4-dodecyloxybenzoic acid was mesomorphic at room temperature displaying a columnar phase (figure 6) and XRD studies of the phase revealed it to be rectangular (Col_r) with $c2mm$ symmetry (table 3). The hydrogen-bonded complex **10** with the 3,4,5-trioxybenzoic acid was also found to be mesomorphic at room temperature displaying a columnar phase that cleared at 59.8°C (figure 7). Unfortunately XRD studies were unsuccessful due to the nature of the compound, which made it impossible to fill the sample capillary, however, from the optical texture of the phase, which contains homeotropic domains, it is believed to be columnar hexagonal.

We next attempted to form hydrogen-bonded complexes of 4-dodecyloxybenzoic acid with the 2,6-disubstituted pyridines **6** to **8**. As for the systems above, pyridine and acid were mixed in THF solution and the solvent removed; final complex formation once more appeared to require subsequent heating. However this time, none of the complexes was mesomorphic, and melting events were broad affairs occurring over some 20 K; there was some evidence of isolated islands of liquid crystallinity, but the temperatures corresponded to those of the free acid. We can be confident that some complexation had occurred as the starting pyridines were almost colourless, while the hydrogen-bonded complexes were a definite yellow. This bathochromic shift is due to partial proton transfer to the pyridine nitrogen, which acts to stabilize the LUMO of this push-pull chromophore, an effect that we have reported previously [12]. The lack of mesomorphism we then attribute to the extra steric strain around the cavity in which the pyridine nitrogen is found, causing the two styryl groups to twist right out of plane, destroying the anisotropy of the complex and thus suppressing mesomorphism. We also conclude that

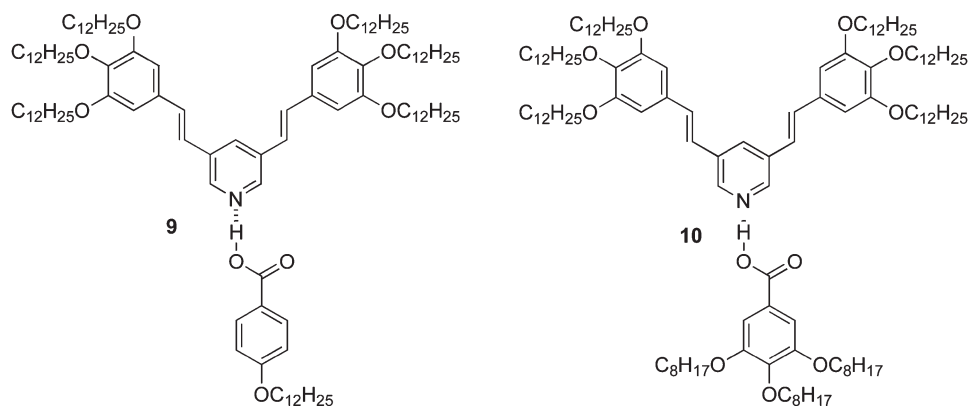


Figure 5. Hydrogen-bonded complexes **9** and **10**.

Table 2. Mesomorphism of the hydrogen-bonded complexes (**9** and **10**).

Compound	Transition	$T/^\circ\text{C}$	$\Delta H/\text{kJ mol}^{-1}$	$\Delta S/\text{JK}^{-1}\text{mol}^{-1}$
9	$\text{Col}_r \rightarrow \text{I}$	69.4	8.4	24
10	$\text{Col}_h \rightarrow \text{I}$	59.8	9.8	30

while complexation does indeed occur in the solid state, on melting the situation is less clear cut and there is some decomplexation — an effect we have observed previously [13]. This is also consistent with a sterically strained system.

3.3. Metal complexes

Notwithstanding the disappointing results obtained with the hydrogen-bonded complexes of the 2,6-disubstituted pyridines, we pursued the formation of metal complexes, and ligands **6**, **7** and **8** were first complexed with silver(I) triflate. Complex $[\text{Ag}(\mathbf{6})_2][\text{OTf}]$ was recovered but could not be obtained in analytical purity whereas, surprisingly, complexation of **7** was unsuccessful since only the free ligand was recovered after several attempts. Better purity was achieved, however, for complex $[\text{Ag}(\mathbf{8})_2][\text{OTf}]$ and POM studies revealed the presence of a mesophase from the melting point at 40°C until it cleared to the isotropic liquid at 58°C . On cooling from the isotropic a rather viscous phase was observed, the texture of which is shown in figure 8, and is assigned as columnar. X-Ray studies of these silver complexes have not been possible.

Ligands **6**, **7** and **8** were then complexed with silver(I) dodecylsulphate using a 2:1 ratio of ligand:silver, and of

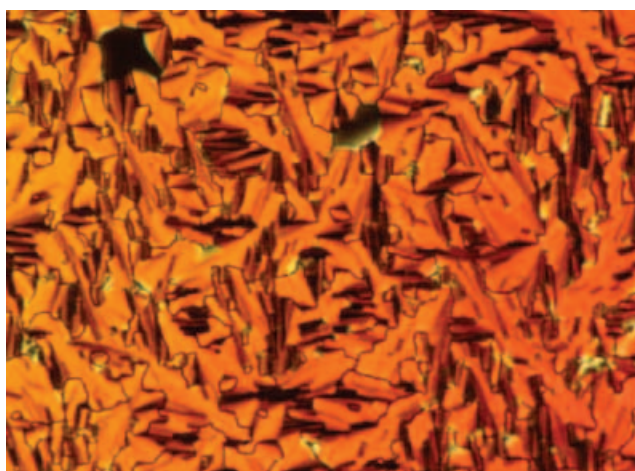


Figure 6. Photomicrograph of the optical texture of the Col_r phase of the hydrogen-bonded complex **9** at 61.7°C on cooling from the isotropic phase.

Table 3. X-Ray diffraction results for the hydrogen-bonded complex **9**.

$T/^\circ\text{C}$	$d_{\text{obs}}/\text{\AA}$	hk	Structural data
55	30.5	11	$a=48.4 \text{ \AA}$
	24.2	20	$b=39.2 \text{ \AA}$
			$S=1896 \text{ \AA}^2$
65	30.0	11	$a=47.7 \text{ \AA}$
	23.9	20	$b=38.6 \text{ \AA}$
			$S=1840 \text{ \AA}^2$

these, only the complex $[\text{Ag}(\mathbf{8})_2][\text{DOS}]$ was recovered successfully. The complex was studied by POM and a mesophase was observed from the melting point at 43°C , until the clearing point, 95°C . On cooling from the isotropic phase, the texture shown in figure 9 was observed for the mesophase and it was characterized as columnar.

Previous investigations of silver(I) dodecylsulphate complexes of 3,4-dialkoxy-4'-stilbazoles suggested that it is possible to form a 1:1 ligand:silver complex [14], thus, attempts to prepare such complexes of ligands **6** to **8** were performed; two of the complexes were recovered with satisfactory purity. Liquid crystal behaviour was observed by POM for $[\text{Ag}(\mathbf{6})][\text{DOS}]$ between 76 and 92°C , and for complex $[\text{Ag}(\mathbf{8})][\text{DOS}]$ between 30 and 98°C . Both of the phases were characterized as columnar (figure 10).

The silver(I) complexes of ligand **8** behave very differently from the related silver(I) complexes of ligand **1c**. Thus, the crystal phase of complex $[\text{Ag}(\mathbf{8})_2][\text{DOS}]$ is destabilized by 17°C compared with the complex $[\text{Ag}(\mathbf{1c})_2][\text{DOS}]$ and the columnar phase is destabilized by 36°C . The destabilization of the crystal phase of the triflate complex $[\text{Ag}(\mathbf{8})_2][\text{OTf}]$ compared with the complex $[\text{Ag}(\mathbf{1c})_2][\text{OTf}]$ is only 7°C , but the clearing

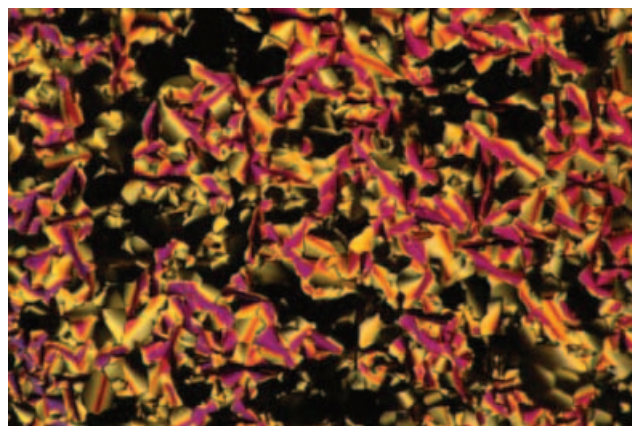


Figure 7. Photomicrograph of the optical texture of the Col_r phase of hydrogen-bonded complex **10** at 53.8°C on cooling from the isotropic phase.

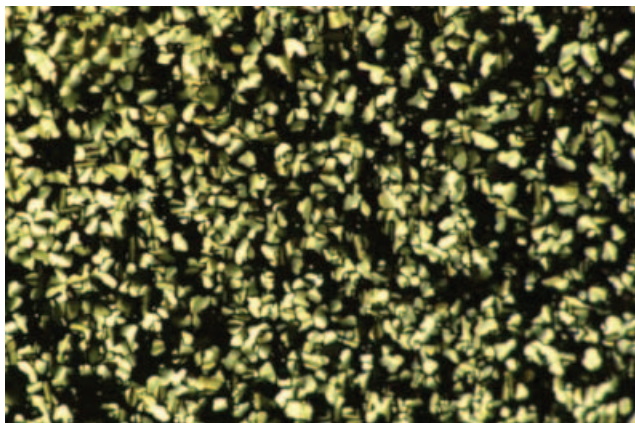


Figure 8. Optical texture of the columnar phase displayed by $[\text{Ag}(\mathbf{8})_2][\text{OTf}]$ at 44°C on cooling from the isotropic liquid.

point of the former complex is 127°C below that of the latter complex. The reason for the destabilization of the columnar phase of the complexes of ligand **8** is likely to be the difficulty of approach to the metal experienced by this ligand compared with ligands **1**. Thus, whereas two ligands **1** can readily approach the metal and form what will be a large, planar disc, a similar situation for ligand **8** is impossible as the two pyridine rings cannot end up co-planar, leading to a twisted situation (figure 11). As drawn, figure 11(b) implies that the two ligands will be at 90° to one another. However, more likely we feel is that the angle will be flattened out as far as possible and that twisting around the various bonds in the styryl link would also occur cooperatively to lead to a final structure that is relatively planar. We believe that this has to be the case, for while the columnar phases are destabilized when the 2,6-disubstituted ligands are used, they are not suppressed entirely which would be the case if the ligands did adopt a mutual 90° angle.

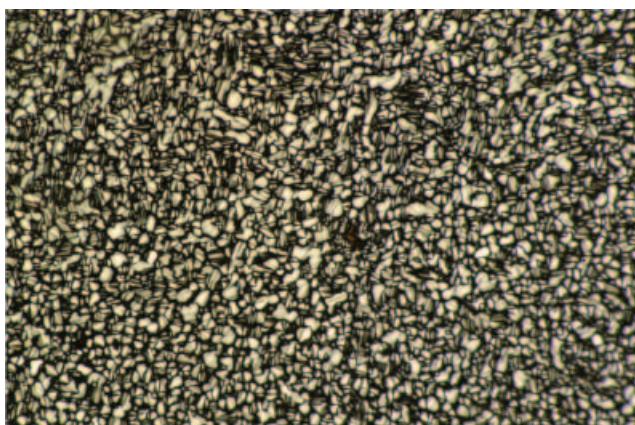


Figure 9. Optical texture of the columnar phase displayed by $[\text{Ag}(\mathbf{8})_2][\text{DOS}]$ at 74°C on cooling from the isotropic liquid.

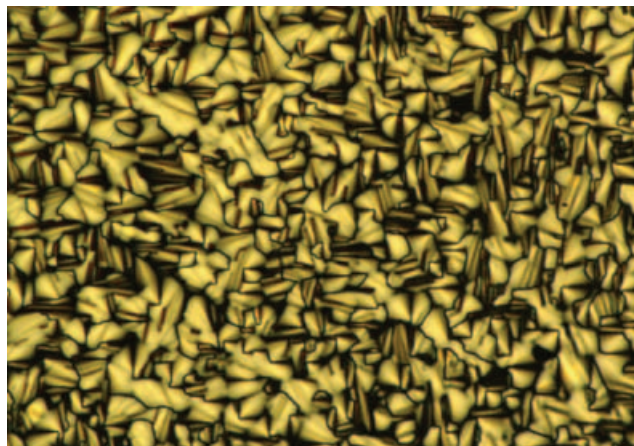


Figure 10. Optical texture of the columnar phase displayed by $[\text{Ag}(\mathbf{6})][\text{DOS}]$ at 91°C on cooling from the isotropic liquid.

The clearing point of the columnar phase displayed by the 1:1 ligand:metal complex $[\text{Ag}(\mathbf{8})][\text{DOS}]$ is curiously similar to the clearing point of the 2:1 complex $[\text{Ag}(\mathbf{8})_2][\text{DOS}]$, but the temperature range of the columnar phase of the former is slightly greater since the melting point is 13°C below that of the latter.

Comparing $[\text{Ag}(\mathbf{8})_2][\text{DOS}]$ with $[\text{Ag}(\mathbf{8})_2][\text{OTf}]$, this time it is the columnar phase of the dodecylsulphate complex that is far more stable, since both complexes melt at *c.* 40°C , but the clearing point of the dodecylsulphate complex was 37°C higher than that of the triflate complex. This is very different from the behaviour of any of the silver(I) dodecylsulphate and triflate complexes that have been investigated previously, where it is always the mesophase of the triflate complex that is found at higher temperatures. We believe that this is an effect related to the ability of the two ligands to twist to give as planar a complex as possible, and that the very much greater destabilization of the columnar phase in the triflate complex suggests that in this system, the ligand rearrangement is much less favourable.

Palladium(II) dichloride complexes of ligands **6** to **8** were also prepared and were purified successfully, but none was mesomorphic. Thus, they melted straight to the isotropic liquid at 107°C ($[\text{PdCl}_2(\mathbf{6})_2]$) and 53.5°C ($[\text{PdCl}_2(\mathbf{7})_2]$), while complex $[\text{PdCl}_2(\mathbf{8})_2]$ was molten at room temperature. Dichloroplatinum(II) congeners were also prepared, but none could be obtained in analytical purity.

4. Conclusion

We have further demonstrated the utility of the Siegrist reaction in preparing mesogenic ligands and have shown how relatively subtle isomeric changes can have

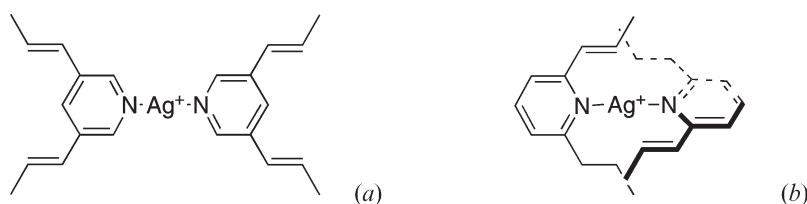


Figure 11. Illustration to show the difference in ease of approach to a metal centre of the 3,5-disubstituted ligands (a) compared with the 2,6-disubstituted ligands (b).

a significant effect on the ability of the ligands to form complexes.

5. Experimental

5.1. Preparation of the hydrogen-bonded complex 9

The preparation of the hydrogen-bonded complex with 4-dodecyloxybenzoic acid (**9**) will be described. Complex **10** was made in the same way but 4-dodecyloxybenzoic acid was replaced with 3,4,5-triocytyloxybenzoic acid.

3,5-Di(3,4,5-tridodecyloxyphenylvinyl)pyridine (**8**) (163.70 mg, 0.1178 mmol) was dissolved in THF under N₂. 4-Dodecyloxybenzoic (36.17 mg, 0.1178 mmol) was dissolved in THF under N₂ and was slowly added to the solution of **8**. The mixture was stirred at room temperature under N₂ for 1 h and the solvent was then removed *in vacuo* leaving a waxy, yellow solid (198 mg, 0.117 mmol, 100%). Purity was checked by elemental analysis

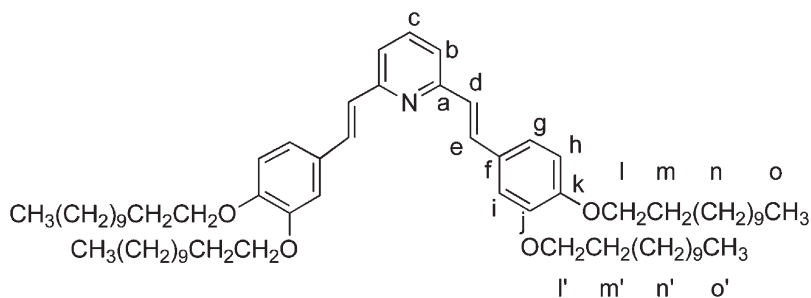
5.2. Preparation of 2,6-di(3',4',-didodecyloxystyryl)pyridine 6

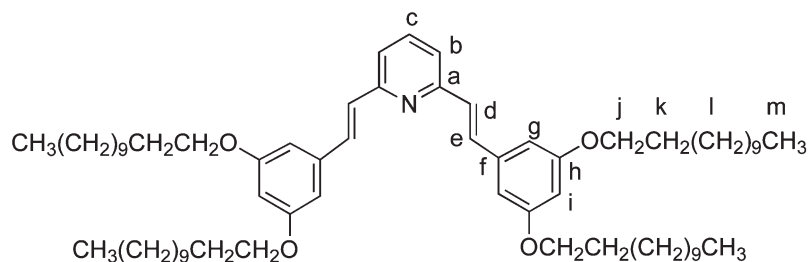
2,6-Di(3',5'-didodecyloxystyryl)pyridine (**7**) and 2,6-di(3',4',5'-tridodecyloxystyryl)pyridine (**8**) were prepared in the same way by using the appropriate benzylidene aniline. 3,4-Didodecyloxybenzylidene aniline (3.0 g, 5.46 mmol) was dissolved in DMF (20 cm³) on heating to 50°C. 2,6-Lutidine (0.28 g, 2.60 mmol) was added and the system was flushed with N₂. Potassium-*t*-butoxide (2.54 g, 20.8 mmol) was added in fractions and the solution became dark red. The system was flushed again with N₂ and was heated at 80°C with stirring for 6 h. After cooling the reaction mixture, HCl (10% solution) was added until pH=7. Water (100 cm³) was added follow by DCM (150 cm³) and the organic phase was separated, washed with aqueous NaHCO₃ (saturated, 100 cm³) and water (100 cm³). After drying over Na₂SO₄, the solvent was removed *in vacuo*. The product was purified by Soxhlet extraction into hexane and a colourless solid was recovered after crystallization (2.26 g, 85%). 2,6-Di(3,5-didodecyloxyphenylvinyl)pyridine (**6**) and 2,6-di(3,4,5-tridodecyloxyphenylvinyl)pyridine (**7**) were purified by column chromatography on silica gel with the eluant mixtures DCM:hexane (1:1) and DCM:hexane (3:2) respectively; a few drops of triethylamine were added to the solvent system to prevent the product sticking to the column.

¹H NMR (300 MHz, CDCl₃): δ=7.63 (1H, t, H_c, ³J_{HH}=7.5 Hz), 7.61 (2H, AB, H_d, J=16.5 Hz), 7.27 (2H, d, H_b, ³J_{HH}=7.5 Hz), 7.20 (2H, d, H_i, ⁴J_{HH}=1.5 Hz), 7.13 (2H, dd, H_g, ³J_{HH}=8.4 Hz, ⁴J_{HH}=1.5 Hz), 7.08

Table 4. Analytical data for the hydrogen-bonded complexes.

Complex	Calculated (found)%		
	C	H	N
9	79.3 (79.6)	11.4 (12.4)	0.8 (0.6)
10	78.6 (78.6)	11.5 (11.8)	0.7 (0.5)





(2H, AB, He, $J=16.5$ Hz) 6.88 (2H, d, Hh, $^3J_{\text{HH}}=8.4$ Hz), 4.07 (4H, t, Hl', $^3J_{\text{HH}}=6.6$ Hz), 4.04 (4H, t, Hl, $^3J_{\text{HH}}=6.6$ Hz), 1.86 (8H, m, Hm, Hm'), 1.42 (72H, m, Hn, Hn'), 0.89 (12H, m, Ho, Ho'). ^{13}C NMR (75.46 MHz, CD_2Cl_2): $\delta=156.1$ (a), 150.1 (j), 149.6 (k) 137.2 (c), 133.1 (d), 130.2 (e), 126.5 (f), 121.4 (b), 119.8 (g), 113.8 (h), 112.1 (i), 69.7 (l), 69.6 (l'), 32.3, 30.1 30.0, 29.9, 29.8, 29.7, 26.5, 26.4, 23.1 (m, n, m', n'), 14.5 (o, o'). Yield 85%, m.p. 84°C. Elemental analysis, % expected (% found) C: 81.2 (81.2), H: 11.2 (11.1), N: 1.4 (1.3).

^1H NMR (300 MHz, CDCl_3): $\delta=7.65$ (1H, t, Hc, $^3J_{\text{HH}}=7.5$ Hz), 7.61 (2H, AB, Hd, $J=16.0$ Hz), 7.28 (2H, d, Hb, $^3J_{\text{HH}}=7.5$ Hz), 7.18 (2H, AB, He, $J=16.0$ Hz), 6.76 (4H, d, Hg, $^4J_{\text{HH}}=2.1$ Hz), 6.44 (2H, t, Hi, $^4J_{\text{HH}}=2.1$ Hz), 3.99 (8H, t, Hj, $^3J_{\text{HH}}=6.6$ Hz), 1.81 (8H, m, Hk), 1.39 (72H, m, Hl), 0.89 (12H, t, Hm, $^3J_{\text{HH}}=6.7$ Hz). ^{13}C NMR (75.46 MHz, CD_2Cl_2): $\delta=160.9$ (h), 155.7 (a), 138.9 (f), 137.3 (c), 133.4 (d), 129.0 (e), 120.7 (b), 106.0 (g), 102.2 (i), 68.5 (j), 32.3, 30.1, 30.0, 29.8, 29.7, 26.5, 23.1 (k, l), 14.5 (m). Yield 61%, m.p. 64°C. Elemental analysis, % expected (% found) C: 81.2 (81.3), H: 11.2 (11.1), N: 1.4 (1.3).

^1H NMR (400 MHz, CDCl_3): $\delta=7.65$ (1H, t, Hc, $^3J_{\text{HH}}=7.8$ Hz), 7.55 (2H, AB, Hd, $J=16.2$ Hz), 7.31 (2H, d, Hb, $^3J_{\text{HH}}=7.8$ Hz), 7.11 (2H, AB, He, $J=16.1$ Hz), 6.84 (4H, s, Hg), 4.05 (8H, t, Hj', $^3J_{\text{HH}}=6.5$ Hz), 4.01 (4H, t, Hj, $^3J_{\text{HH}}=7.8$ Hz), 1.82 (12H, m, Hk, Hk'), 1.41 (108H, m, Hl, Hl'), 0.91 (18H, m, Hm, Hm'). ^{13}C NMR (100.61 MHz, CD_2Cl_2): $\delta=155.6$ (a), 153.3 (h), 138.8 (i), 136.8 (c), 133.0 (d), 131.9 (f), 127.5 (e), 119.6 (b), 105.7

(g), 73.6(j), 69.1 (j'), 32.0, 30.4, 30.0, 29.8, 29.7, 29.6, 29.5, 29.4, 29.3, 26.1, 22.7 (k, l, k', l'), 14.2 (m, m'). Yield 65%, m.p. 60°C. Elemental analysis, % expected (% found) C: 80.4 (80.0), H: 11.7 (12.7), N: 1.0 (0.8).

5.3. Preparation of silver complexes with two ligands

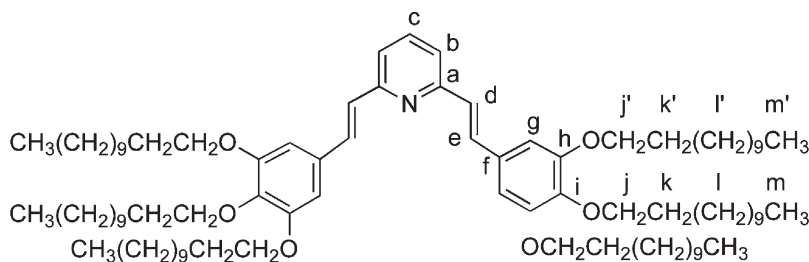
A solution of the ligand (0.109 mmol) in CH_2Cl_2 (10 cm^3) was added dropwise to a suspension of a silver salt AgX (0.054 mmol) in the same solvent (10–20 cm^3) and a change of colour to deep yellow was observed. The reaction mixture was stirred for 6 h (triflates) or 24 h (DOS compounds) in the absence of light. Then the yellow solution was filtered through celite and the solvent was partially removed. A yellow/orange solid (OTf/DOS) was obtained from hexane/acetone after refrigerating the solution overnight.

$[\text{Ag}(\mathbf{8})_2]\text{OTf}$: yield 70%. Anal: % expected (% found), C 74.0 (75.2), H 10.7 (11.1), N 0.9 (1.1).

$[\text{Ag}(\mathbf{8})_2][\text{DOS}]$: yield 82%. Anal: % expected (% found): C 75.45 (76.60), H 11.10 (11.52), N 0.89 (0.94).

5.4. Preparation of silver complexes with one ligand

A solution of the ligand (0.101 mmol) in CH_2Cl_2 (10 cm^3) was added dropwise to a suspension of AgDOS (0.010 mmol) in the same solvent (10 cm^3). The reaction mixture was stirred for 24 h. The yellow solution was filtered through celite and the solvent partially removed. The addition of Et_2O /acetone led to the precipitation of a yellow solid after several hours



refrigeration. It was filtered, washed with acetone and dried in vacuum. In some cases, the solids so obtained were recrystallized from hexane/acetone.

[Ag(6)][DOS]: yield 42%. Anal: % expected (% found) for $\text{AgC}_{81}\text{H}_{138}\text{NO}_8\text{S}$: C 69.8 (69.9), H 10.0 (10.6), N 1.0 (0.7).

[Ag(8)][DOS]: yield 61%. Anal: % expected (% found): C 71.5 (71.1), H 10.6 (10.3), N 0.8 (0.7).

Acknowledgements

This work was supported by Comunidad de Madrid, by contract No. GR/MAT/0511/2004 and by a postdoctoral fellowship (M.C.T.), by the UK EPSRC (D.M.H. and H.L.N.) and by the Collège Doctoral Européen de Strasbourg (D.M.H.). Helpful discussions with Dr Daniel Guillon (IPCMS, Strasbourg) are acknowledged gratefully.

References

- [1] D.W. Bruce. *Adv. Inorg. Chem.*, **52**, 151 (2001).
- [2] D.W. Bruce. *Acc. chem. Res.*, **33**, 831 (2000).
- [3] H.L. Nguyen, P.N. Horton, M.B. Hursthouse, A.C. Legon, D.W. Bruce. *J. Am. chem. Soc.*, **126**, 16 (2004).
- [4] D.W. Bruce, A. Thornton. *Mol. Cryst., liq. Cryst.*, **231**, 253 (1993).
- [5] (a) J.E. Wong, B. Donnio, D.W. Bruce, T.H. Richardson. *Appl. surface Sci.*, **246**, 451 (2005); (b) J.E. Wong, D.W. Bruce, T.H. Richardson. *Synth. Met.*, **148**, 11 (2005).
- [6] D.M. Huck, H.L. Nguyen, B. Donnio, D.W. Bruce. *Liq. Cryst.*, **31**, 503 (2004).
- [7] R. Amaranatha Reddy, C. Tschierske. *J. mater. Chem.*, **16**, 907 (2006).
- [8] A.E. Siegrist. *Helv. Chim. Acta.*, **50**, 1399 (1967).
- [9] E. Gorecka, D. Pocięcha, J. Mieczkowski, J. Matraszek, D. Guillon, B. Donnio. *J. Am. chem. Soc.*, **124**, 15946 (2004).
- [10] (a) K. Willis, J.E. Luckhurst, D.J. Price, J.M.J. Fréchet, H. Kihara, T. Kato, G. Ungar, D.W. Bruce. *Liq. Cryst.*, **21**, 585 (1996); (b) T. Kato, J.M.J. Fréchet. *J. Am. chem. Soc.*, **111**, 8533 (1989); (c) U. Kumar, T. Kato, J.M.J. Fréchet. *J. Am. chem. Soc.*, **114**, 6630 (1992); (d) D.W. Bruce, D.J. Price. *Adv. Mater. opt. Electron.*, **4**, 273 (1994); (e) K. Willis, D.J. Price, H. Adams, G. Ungar, D.W. Bruce. *J. mater. Chem.*, **5**, 2195 (1995).
- [11] K. Willis, J.E. Luckhurst, D.J. Price, J.M.J. Fréchet, H. Kihara, T. Kato, G. Ungar, D.W. Bruce. *Liq. Cryst.*, **21**, 585 (1996).
- [12] D.J. Price, T. Richardson, D.W. Bruce. *Chem. Commun.*, 1911 (1995).
- [13] D.J. Price, H. Adams, D.W. Bruce. *Mol. Cryst., liq. Cryst.*, **289**, 127 (1996).
- [14] B. Donnio, B. Heinrich, T. Gulik-Krzywicki, H. Delacroix, D. Guillon, D.W. Bruce. *Chem. Mater.*, **9**, 2951 (1997).